

Simulative Investigation of Spectral Amplitude Coding Based OCDMA System Using Quantum Logic Gate Code with NAND and Direct Detection Techniques

Teena Sharma^{1*}, Ravi Kumar Maddila¹, and Syed Alwee Aljunid²

¹Department of Electronics and Communication, Malviya National Institute of Technology,
302017 Jaipur, India

²School of Computer and Communication Engineering, University Malaysia Perlis, (UniMAP),
02000 Kuala Perlis, Malaysia

(Received June 19, 2019 : revised August 18, 2019 : accepted September 6, 2019)

Spectral Amplitude Coding Optical Code Division Multiple Access (SAC OCDMA) is an advanced technique in asynchronous environments. This paper proposes design and implementation of a novel quantum logic gate (QLG) code, with code construction algorithm generated without following any code mapping procedures for SAC system. The proposed code has a unitary matrices property with maximum overlap of one chip for various clients and no overlaps in spectra for the rest of the subscribers. Results indicate that a single algorithm produces the same length increment for codes with weight greater than two and follows the same signal to noise ratio (SNR) and bit error rate (BER) calculations for a higher number of users. This paper further examines the performance of a QLG code based SAC-OCDMA system with NAND and direct detection techniques. BER analysis was carried out for the proposed code and results were compared with existing MDW, RD and GMP codes. We demonstrate that the QLG code based system performs better in terms of cardinality, which is followed by improved BER. Numerical analysis reveals that for error free transmission (10^{-9}), the suggested code supports approximately 170 users with code weight 4. Our results also conclude that the proposed code provides improvement in the code construction, cross-correlation and minimization of noises.

Keywords : SAC OCDMA, Quantum logic gate, Detection technique, Phase induced intensity noise
OCIS codes : (060.0060) Fiber optics and optical communications; (060.2310) Fiber optics; (060.4510) Optical communications

I. INTRODUCTION

Over last decade, Optical Code Division Multiple Access (OCDMA) has been used as a promising technology for optical access networks, and it offers precedence for asynchronous access, multiple numbers of users, high reliability and flexibility, high Quality of Service (QoS), simple network architecture, easy network management and high security [1]. However, system performance for OCDMA networks degrades due to extensive clients responsible for Multiple Access Interference (MAI) and other parameters such as thermal noise, shot noise and Phase Induced Intensity Noise (PIIN). Among all parameters PIIN is the

most dominant noise for optical networks [2]. Further limitation of system data rate occurs due to MAI, which constrains the system bandwidth, followed by system noise increment and high bit error rates [3]. For an OCDMA system, the optical communication channel may be either fiber optic or wireless Free Space Optics (FSO). OCDMA is one of the leaders in optical communication due to its capability in handling various types of data traffic and its huge bandwidth which makes it a suitable candidate for multimedia applications, especially triple play services with constant weight and variable weight code families [4]. In addition, data can be transmitted seamlessly while easily managing and controlling networks. The second approach

*Corresponding author: 2013rec9539@mnit.ac.in, ORCID 0000-0002-9002-0595

Color versions of one or more of the figures in this paper are available online.



This is an Open Access article distributed under the terms of the Creative Commons Attribution Non-Commercial License (<http://creativecommons.org/licenses/by-nc/4.0/>) which permits unrestricted non-commercial use, distribution, and reproduction in any medium, provided the original work is properly cited.

can be an alternative solution with its low maintenance cost of optical networks and deployment time but with a limitation of small distance especially in rural and remote areas [5]. OCDMA is preferred in conjunction with Spectral Amplitude Coding (SAC) for optical networking because of its efficient MAI dispensing capabilities due to zero and ideal cross correlation coding approaches and efficient detection methods such as complementary subtraction and direct detection [6, 7]. Balanced detection methods can fully eliminate MAI by subtracting interfering chips of code-words using optical subtractors and two photodiodes (PDs), placed in balanced mode [8]. The direct detection technique only deals with clean chips, thus PIIN is removed by using lesser filter components. Unfortunately, MAI is not completely eliminated as full weight present in user code is not used at the receiver. In this respect, NAND subtraction detection provides better performance while dealing with MAI efficiently as compared to complementary, AND, and XOR, due to higher weights in user code resulting in high signal power and quality [9, 10].

Various code sequences reported previously such as MD, MDW, MQC, FCC, RD, DCS, GMP and EDW possessing fixed and zero cross-correlation properties have limitations in terms of large code length, complex code construction, code cardinality and high cross-correlation compelling its use only for short distance communication specifically for Local Area Network (LAN) and Fiber to the Home (FTTH) applications [11, 12]. In addition, SAC systems implemented with incoherent sources have limitations in terms of achievable data rates, distance and high intensity noise due to the broad spectrum of incoherent white light sources. Use of multi-wavelength laser sources provide a cost effective solution with desirable system performance but its choice depends on many factors such as reliability requirements, target applications and related performance of the communication system [13]. With advancement in technology, hybridization of the multi array laser with a white light source is considered as a potential approach for improving OCDMA performance [14]. On the contrary, recent studies revealed that 2D codes have substantial potential over 1D code due to their efficient bandwidth utilization with higher transmission capabilities and better performance in terms of increased cardinality with spectral density expansion at the cost of high speed electronic devices [15].

Some 1D code families have limitations of code mapping. The mapping technique is used to increase the number of users for each weight, if needed, in which first a basic matrix is constructed and it is repeated diagonally to increase the number of users [16]. Increment of code length is not fixed and it is based on the size of the basic matrix and the demanded number of extra subscribers because of mapping procedures [17, 18]. For example, if code length for 4 users is 10 then for 5 users it is 15, for 6 users it is 20 and so on (increment of 5 for each user). In addition, the codes utilizing code mapping technique for

their design present limitation on the supportable number of client due to occurrence of variable cross-correlation issues with increase in users, which constrain system performance due to MAI [19, 20].

As a consequence, the main objective of this study is to design optical code which is independent of code mapping technique to maintain fixed code length increment for additional subscribers and also a single code construction algorithm that can be used for all weights higher than 2. The proposed code algorithm is designed from mathematical operation of classical quantum logic. Since code matrices are based on reverse quantum logic gates derived eigenvalues, therefore, implemented method of code design was different from that of conventional code construction techniques. In particular, we have implemented QLG code for higher number of users in the OCDMA environment by considering the most practical optical signal intensity detection techniques such as NAND and Direct Detection (DD). We expected that the proposed code could provide more flexibility in selection of code weight, number of subscribers and simple code construction approaches when compared to previous codes. The overall study was organized as follows: Section 2 includes QLG code construction. Section 3 discusses performance analysis of the proposed code in the SAC-OCDMA framework followed by comparative analysis with existing codes in Section 4. Finally, conclusions were drawn in Section 5.

II. QUANTUM LOGIC GATE CODE CONSTRUCTION METHOD

2.1. Code Construction Step

The proposed effective code construction by utilizing the Quantum Logic Gate (QLG) method is summarized in the following steps,

- Step 1: Construct matrices using the weight (I) and the number of users (K).
- Step 2: Set the number of rows and columns of matrix value according to $(I \times K)$.
- Step 3: Diagonal sequences are computed by using the QLG method.
- Step 4: The total combination of QLG sequences is $(K \times N)$.

2.2. Code Construction Algorithm

Quantum logic gates are represented by unitary matrices and work on spaces of a couple of qubits. The quantity of qubits in the information and yield of the gate must be equivalent. The code length of the QLG code operating on a single qubit is always minimum but if the quantum logic gate operates on a double qubit, then the code length will be maximized. Based on these ideas, in the proposed code the idea of a reverse quantum logic gate is used as an operation, not as a quantum gate. The vector representation

of the proposed code using a single qubit is given below,

$$R1|0\rangle + R2|1\rangle = \begin{bmatrix} R1 \\ R2 \end{bmatrix} \quad (1)$$

Where R1 and R2 signify rows of basic matrix M which contains values 1 or 0. Basic matrix (M) of dimensions $2 \times (I-1)$ of code includes the weight value (I) and the number of subscribers (K) in the diagonals of the matrix.

$$M = \begin{bmatrix} R1 \\ R2 \end{bmatrix} = \frac{1}{2} \begin{bmatrix} 1+K & 1-I \\ 1-I & 1-K \end{bmatrix} \quad (2)$$

H represents matrix of size $K \times N$ for K subscribers which show the total code set. The development of H includes 3 stages, at first make a intermediary matrix of H^* then M is reshaped (K-1) times in H^* as demonstrated in Eq. (3),

$$H^* = \begin{bmatrix} R1 & \dots & \dots & \dots & \dots & \dots \\ R2 & R1 & \dots & \dots & \dots & \vdots \\ \vdots & R2 & R1 & \dots & \dots & \vdots \\ \vdots & \vdots & \vdots & \ddots & \ddots & \vdots \\ \vdots & \vdots & \vdots & \ddots & R1 & \vdots \\ \dots & \dots & \dots & \dots & R2 & \dots \end{bmatrix} \quad (3)$$

Basic matrix rows R1 and R2 are added to the last column of matrix H^* by filling the remaining columns.

$$H^{**} = \begin{bmatrix} R1 & \dots & \dots & \dots & \dots & R2 \\ R2 & R1 & \dots & \dots & \dots & \vdots \\ \vdots & R2 & R1 & \dots & \dots & \vdots \\ \vdots & \vdots & \vdots & \ddots & \ddots & \vdots \\ \vdots & \vdots & \vdots & \ddots & R1 & \vdots \\ \dots & \dots & \dots & \dots & R2 & R1 \end{bmatrix}_{K \times N} \quad (4)$$

Lastly the total code set is created by topping off the unfilled spots with zeros

$$H = \begin{bmatrix} R1 & 0 & 0 & \dots & \dots & R2 \\ R2 & R1 & 0 & \dots & \dots & 0 \\ 0 & R2 & 0 & \ddots & \ddots & \vdots \\ \vdots & \vdots & \vdots & \ddots & \ddots & \vdots \\ \vdots & \vdots & \vdots & \ddots & \ddots & \vdots \\ 0 & 0 & 0 & \dots & \dots & R1 \end{bmatrix}_{K \times N} \quad (5)$$

The QLG code is characterised by parameters (N, I, $\lambda_c = 1$), where N is the number of total chips in the code word

or code length, I signifies the weight value (time chips having value 1) and λ_c is the in-phase cross-correlation

2.3. Code Example Utilizing Even Weight Value (I = 4):

Step-1 Let the number of subscribers be $K=3$. Code length is ascertained below,

$$N = K \times (I-1) = 3 \times (4-1) = 3 \times 3 = 9$$

Step-2 Size of matrix is characterized as $2 \times (I-1) = 2 \times (4-1) = 2 \times 3$. M is created as,

$$\begin{aligned} M &= \begin{bmatrix} R1 \\ R2 \end{bmatrix} = \frac{1}{2} \begin{bmatrix} 1+K & 1-I & 1+K \\ 1-I & 1-K & 1-I \end{bmatrix} \\ &= \frac{1}{2} \begin{bmatrix} 1+3 & 1-4 & 1+3 \\ 1-4 & 1-3 & 1-4 \end{bmatrix} \\ &= \begin{bmatrix} 2 & -1.5 & 2 \\ -1.5 & -1 & -1.5 \end{bmatrix} \end{aligned}$$

Step-3 The generated matrix contains numeric values but the system requires binary values as the input. Thus using reverse quantum logic gate operation ($-1 \Rightarrow 1$; $1 \Rightarrow 0$), negative value is replaced by '1' and positive value by '0',

$$= \begin{bmatrix} 2 \rightarrow [0] & -1.5 \rightarrow [1] & 2 \rightarrow [0] \\ -1.5 \rightarrow [1] & -1 \rightarrow [1] & -1.5 \rightarrow [1] \end{bmatrix}$$

The matrix is defined as,

$$M = \begin{bmatrix} R1 \\ R2 \end{bmatrix} = \begin{bmatrix} 0 & 1 & 0 \\ 1 & 1 & 1 \end{bmatrix}_{2 \times 3}$$

Step-4 M is reshaped multiple times as,

$$H^* = \begin{bmatrix} 0 & 1 & 0 & \dots & \dots & \dots \\ 1 & 1 & 1 & 0 & 1 & 0 \\ \dots & \dots & \dots & 1 & 1 & 1 \end{bmatrix}_{K \times N}$$

Step-5 Matrix upper line R1 and lower line R2 are placed in the last and first lines of the last segment as,

$$H^{**} = \begin{bmatrix} 0 & 1 & 0 & \dots & \dots & \dots & 1 & 1 & 1 \\ 1 & 1 & 1 & 0 & 1 & 0 & \dots & \dots & \dots \\ \dots & \dots & \dots & 1 & 1 & 1 & 0 & 1 & 0 \end{bmatrix}_{3 \times 9}$$

Step-6 The remaining spots are loaded up with zeros,

$$H = \begin{bmatrix} 0 & 1 & 0 & 0 & 0 & 0 & 1 & 1 & 1 \\ 1 & 1 & 1 & 0 & 1 & 0 & 0 & 0 & 0 \\ 0 & 0 & 0 & 1 & 1 & 1 & 0 & 1 & 0 \end{bmatrix}_{3 \times 9}$$

TABLE 1. QLG code patterns for (I = 3 and N = 6)

0	1	0	0	1	1
1	1	0	1	0	0
0	0	1	1	0	1

TABLE 2. Code-words possible combination

No. of users (K)	Odd	Even	Odd	Even
Code weight (I)	Odd	Even	Even	Odd

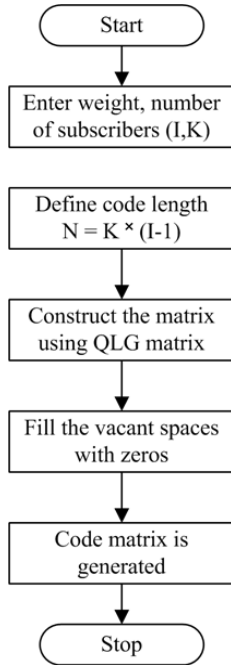


FIG. 1. Flowchart of the QLG code development.

Table 1 depicts code words for 3 users with weight 3 which we have used in our simulation and Table 2 represents four possible sets of code-words for I and K for the proposed code, which shows that QLG code provides flexibility in choosing code weights irrespective of number of users and code length. Figure 1 shows the accompanying strides to be performed for the code.

III. PERFORMANCE ANALYSIS FRAMEWORK

3.1. Gaussian Estimation

We utilized the QLG based Gaussian estimation for BER computation. We made following assumptions for analysis of system BER [13]:

1. Each light source consists of a flat spectrum over a bandwidth $[v_o - \Delta v/2]$ to $[v_o + \Delta v/2]$, where v_o is the optical central frequency and Δv is the optical source bandwidth. Each light source is ideally unpolarized.

2. Each frequency component has identical frequency spectrum width.
3. Received power is the same for each user.
4. Each bit stream is synchronized for each user.

The variance of detector current due to detection of an ideally unpolarized light (thermal source), which is produced by spontaneous emission, can be given as

$$\sigma^2 = \sigma_{sh} + \sigma_{PIIN} + \sigma_{th} \quad (6)$$

$$\sigma^2 = 2eBI + \frac{4BTnKb}{RL} + BI^2\tau_c \quad (7)$$

where σ_{sh} indicates shot noise in the photo-detector, σ_{PIIN} denotes intensity noise σ_{th} indicates thermal noise, I is average photocurrent and τ_c is coherence time of a thermal source.

By utilizing QLG code's properties with fixed cross-correlation ($\lambda_c = 1$), correlation factor can be stated as,

$$\sum_{i=1}^N L_m(i)L_n(i) = \begin{cases} I, & m = n \\ 1, & \text{else} \end{cases} \quad (8)$$

where $L_m(i)$ is the i^{th} element of m^{th} QLG code sequence and is equal to code weight (I) for the same user and CC is 1 for the rest of the users.

The Power Spectral Density (PSD) is composed as [9],

$$V(d) = \frac{P_{sr}}{\Delta v} \sum_{j=1}^j k_j \sum_{i=1}^N L_m(i) \text{set}(p) \quad (9)$$

where P_{sr} is the successful intensity of broad band source at the beneficiary, data bit k_j represents j^{th} client data bit, which is either "1" or "0" and $\text{set}(p)$ is a rectangular function represented as,

$$\text{set}(p) = u \left[v - v_0 - \frac{\Delta v}{2N}(-N + 2i - 2) \right] - u \left[v - v_0 - \frac{\Delta v}{2N}(-N + 2i) \right] = u \left[\frac{\Delta v}{N} \right] \quad (10)$$

where $u(v)$ represents unit step function as stated below;

$$u(v) = \begin{cases} 1, & v \geq 0 \\ 0, & v < 0 \end{cases} \quad (11)$$

Integration of PSD amid one period can be composed as:

$$\int_0^\infty G_1(v)dv = \int_0^\infty \left[\frac{P_{sr}}{\Delta v} \sum_{j=1}^j K_j \sum_{i=1}^N L_m(i) \text{set}(p) \right] dv \quad (12)$$

Eq. (12) can be streamlined as follows:

$$\int_0^{\infty} G_1(v) dv = \frac{P_{sr}}{\Delta v} \left[\sum_{j=1}^j k_j \dots I \cdot \frac{\Delta v}{N} + \sum_{j \neq 1}^j k_j \dots I \cdot \frac{\Delta v}{N} \right] \quad (13)$$

$$\int_0^{\infty} G_1(v) dv = \frac{P_{sr}}{\Delta v} \left[(I+1) \sum_{j=1}^j k_j \dots I \cdot \frac{\Delta v}{N} \right] \quad (14)$$

Mentioned in Eq. (14), is the information bit representing a client that is either “1” or “0”. When all clients are transmitting bit “1”,

$$\left| \sum_{j=1}^j k_j \right| = [k_1 + k_2 + k_3 + \dots + k_{j-1} + k_j] = I$$

After that,

$$\int_0^{\infty} G_1(v) dv = \frac{P_{sr} I (I+1)}{N} \quad (15)$$

The photo diode current **I** is represented as,

$$I = \mathfrak{R} \int_0^{\infty} G_1(v) dv \quad (16)$$

At that point Eq. (16) can be communicated as follows

$$I^2 = \left(\mathfrak{R} \int_0^{\infty} G_1(v) dv \right)^2 = \left(\frac{\mathfrak{R} P_{sr} I (I+1)}{N} \right)^2 \quad (17)$$

Substituting Eq. (17) in Eq. (7), we get:

$$\sigma^2 = \frac{2eB\mathfrak{R}P_{sr}I^2}{N} + \frac{4BT_nK_b}{R_L} + \frac{B(\mathfrak{R}P_{sr}I)^2 \tau_c}{N} \quad (18)$$

As the probability of sending bit “1” for every client is $\frac{1}{2}$, in this way Eq. (18) progresses toward becoming,

$$\sigma^2 = \frac{eB\mathfrak{R}P_{sr}I(I+1)}{N} + \frac{4BT_nK_b}{R_L} + \frac{B(\mathfrak{R}P_{sr}I(I+1))^2}{N} \quad (19)$$

In conclusion taking into account Eq. (17) and Eq. (19), the SNR can be stated as

$$SNR = \left[\frac{\left(\frac{\mathfrak{R}P_{sr}I(I+1)}{N} \right)^2}{\frac{eB\mathfrak{R}P_{sr}I(I+1)}{N} + \frac{4T_nBK_b}{R_L} + \frac{B(\mathfrak{R}P_{sr}I(I+1))^2}{N \times \Delta v}} \right] \quad (20)$$

where P_{sr} is broadband source power, electron charge (e), photodiode responsivity is \mathfrak{R} , B is electrical equivalent noise bandwidth of receiver, N is the number of users, e is electron charge, R_L receiver load resistor, receiver noise temperature is T_n , I is code weight, K_b is Boltzmann’s constant and Δv is the chip spectral width of the broadband light source.

Utilizing Gaussian estimate, the Bit Error Rate can be written as [10]:

$$BER = P_e = \frac{1}{2} \operatorname{erfc} \left(\sqrt{\frac{SNR}{8}} \right) \quad (21)$$

3.2. Simulation Setup

QLG code was implemented in Optisystem software 13 by Optisym™, for 3 users. The simulation setup is shown in Figs. 2 and 3 with NAND and direct detection techniques. The encoder design for both the techniques is the same. The transmitter consists of broadband white light sources, which are mainly white light LEDs, encoder and Mach Zehnder Modulator (MZM). At the beneficiary, the output spectrum of the LED is sliced into six wavelengths. Each sliced chip with a chip spectral width 0.8 nm is modulated according to the given data generated by a pseudo random bit sequence (PRBS) source. Uniform Fiber Bragg Gratings (FBGs) are used for filtering wavelengths. FBG1, FBG2 and FBG3 wavelengths correspond to 1st user (010011 from Table 1) are set to 1550.8 nm, 1553.2 nm and 1554 nm. Similarly for 2nd and 3rd users, FBG’s wavelengths are set to (1500 nm, 1500.8 nm and 1552.4 nm) and (1551.6 nm, 1552.4 nm and 1554 nm). These wavelengths represent code weights in QLG code. Further, MZM is used to modulate user data with the coded sequence. Codes from different customers were joined before moving onto the optical fiber using the multiplexer with its insertion loss 2 dBm. The simulation was carried out for ITU-G 652 standard single mode fiber with fiber length 70 kms.

At the receiver end using NAND subtraction, received signals were sent first into a decoder which consists of two sections, in which the upper section consists of three uniform fiber bragg gratings (FBGs) for each user, acting as an optical filter. It has the same filter structure used in the encoder part. The other section consists of an FBG with the wavelength structure according to NAND function [21]. After filtering, PIN Photo Detector diodes (PD1 and PD2) detected the received signals and the electrical signal in the lower arm is subtracted from that of the upper arm

causing MAI and beat noise mitigation to a larger extent. Finally the received signal was analysed by BER analyser (Fig. 2).

At the receiver using a DD technique, the received signal for each user is passed to filter structures which are set on non-overlapping wavelengths. FBG wavelengths corresponding to the 1st user are set to non-overlapping wavelengths (1553.2 nm and 1554 nm) for each user. Similarly for 2nd and 3rd users, FBG's wavelengths are set to (1500 nm and 1552.4 nm) and (1551.6 nm and 1554 nm). After filtering, signal is detected by single photo detector for each user (Fig. 3). PIIN noise is suppressed on detecting non-overlapping wavelengths therefore the system performance

is improved in terms of BER. Only fewer clean chips are detected by diode detector, which reduces the received power and affects the performance of BER. The DD technique does not use two photo detectors, power splitters and subtractor thus it also provided low cost and less complex receiver architecture due to fewer components as compared to NAND detection method. Full code spectra are transmitted to recover the signature sequence.

Other fiber related parameters such as Polarization Mode Dispersion (PMD) of 0.7 ps/ $\sqrt{\text{km}}$ and chromatic dispersion 18.75 ps/nm-km and attenuation (α) of 0.25 dB/km were set and wavelength dependent non-linear effects (four wave mixing, cross phase modulation and self-phase modulation)

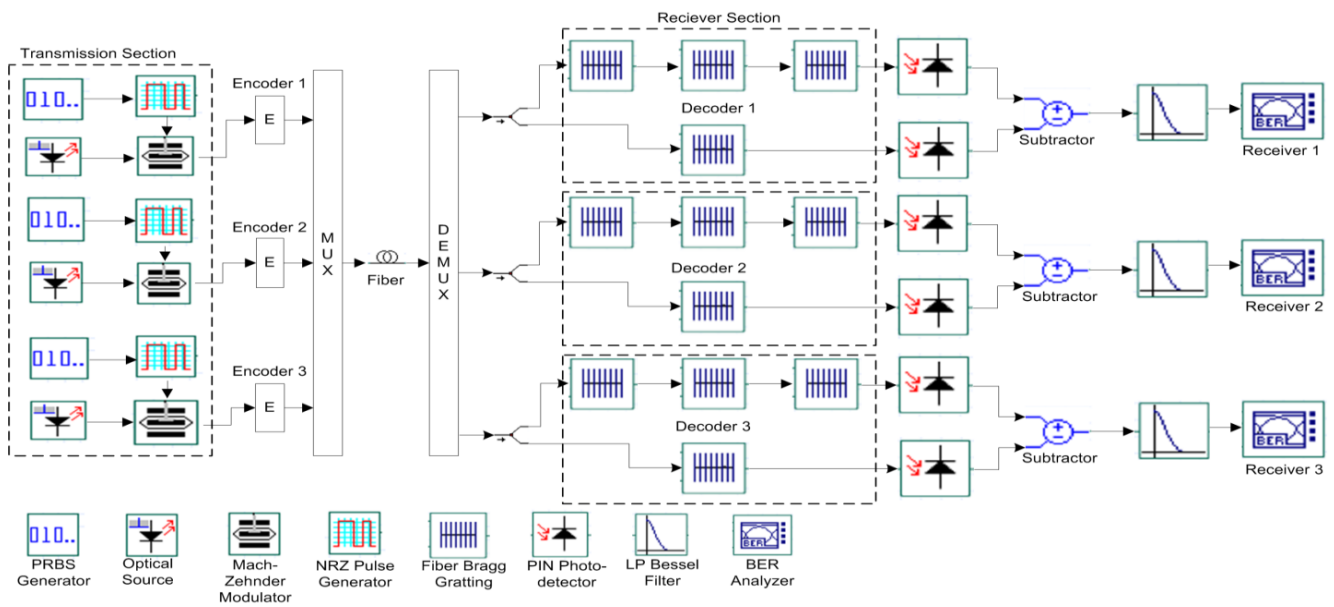


FIG. 2. Simulation setup for SAC system using NAND detection technique.

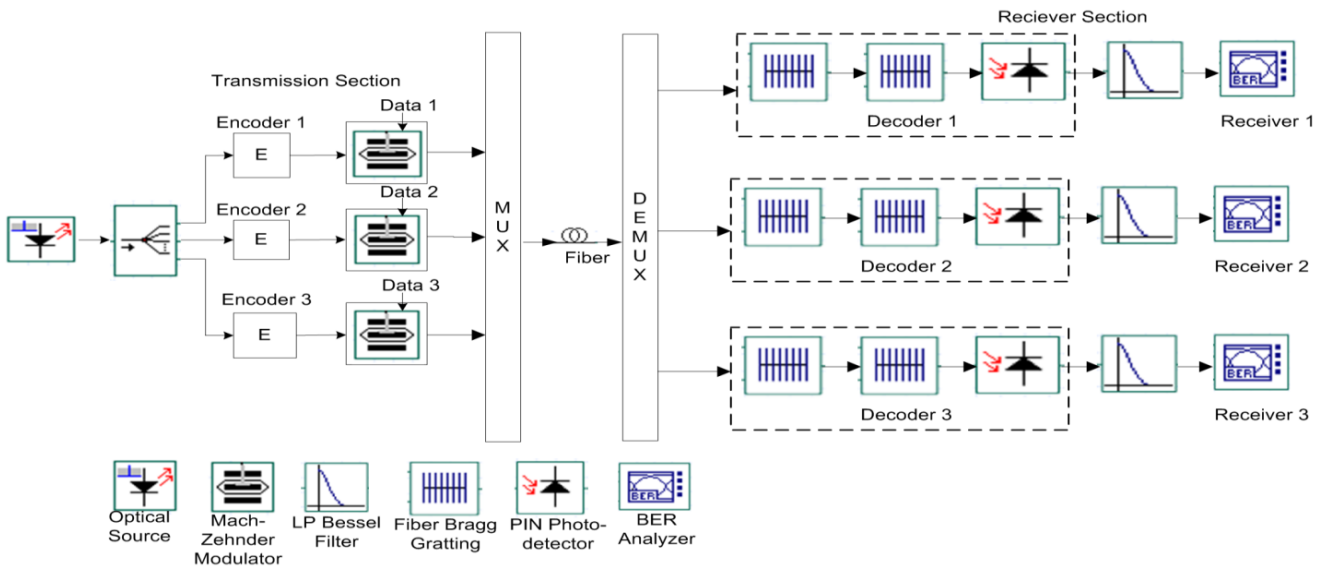


FIG. 3. SAC OCDMA system setup for QLG code using DD technique.

was activated during simulation. The PIN photo diode detector responsivity is set to 1 A/W, dark current of 5 nA and thermal noise of 1.8×10^{-24} W/Hz.

IV. RESULTS AND ANALYSIS

In this section, results are shown for performance evaluation for theoretical and simulation analyses for QLG based on the parameters listed in Table 3 and performance comparison with existing codes is made in Table 4. For all the analysis, Effective Source Power (P_{sr}) was set to -10 dBm and simulation was carried out at 1 Gbp/s bit rates.

Minimum code weight minimized the interference among codes which resulted in improvement in QLG system performance (Fig. 4(a)). As the number of clients increases the quality of the received signal deteriorates due to occurrence of MAI among them. Thus, system SNR and BER degrades. Moreover, system avoided effect of basic matrix size on the BER floor due to development of QLG code without a code mapping technique. It was observed that the system can support 170 users at minimum acceptable BER value of 10^{-9} (Fig. 4(a)). Different weights (I) were considered with existing SAC codes (GMP, RD and MDW) and their performance was compared with QLG code (Fig. 4(b)).

BER values were compared with QLG and existing techniques MDW and RD by taking weight value three ($I = 3$) (Fig. 4(b)). It was observed that supported clients were 60, 110 and 170 for RD, MDW and QLG, respectively, at BER 10^{-9} . However, the performance of QLG was higher due to minimum cross-correlation ($\lambda_c = 1$) when compared with RD ($\lambda_c = 2$) and MDW ($\lambda_c = 1$). Due to smaller code length, high cross-correlation of RD and MDW codes were observed.

Further, for varying weights, the performance of QLG code was compared with RD, MDW and GMP codes (Fig. 4(c)). Results showed that QLG supported higher number of users for fewer weights when compared to existing codes and its performance improved as the code weight increased. Transmitted power increased due to increase in weight, which resulted into low error probability, whereas, resultant number of users for same BER increased due to larger code length (Fig. 4(c)).

TABLE 3. Parameters used for numerical and simulation analysis of QLG based SAC system

Parameters	Value
Electrical bandwidth (B)	311 MHz
Electron charge (e)	1.6×10^{-19}
Effective power of source (P_{sr})	-10 dBm
Operating wavelength (λ_w)	1550 nm
Quantum efficiency of LED (η)	0.6
Broadband source width (Δf)	3.75 THz
Photodiode responsivity (R)	0.75
Boltzmann constant (K_b)	1.38×10^{-23} W/K/Hz
Receiver noise temperature (T_n)	300 K
Load resistor at receiver (R_L)	1030 Ω

Figure 4(d) showed variation between SNR and number of users for varying weights. It was observed that performance of SNR improved due to high code weight values. Since each chip contain 1's (weights) corresponds to the signal power, therefore signal power increased. This resulted in improvement of both SNR and BER performance.

The performance of the SAC system with NAND subtraction and DD techniques using QLG code is demonstrated with eye diagram (Figs. 5(a) and 5(b)). In the case of DD, achieved minimum BER was 3.4×10^{-20} with 10.16 Q factor and for NAND it was 3.10×10^{-13} with 7.14 Q factor (Figs. 5(a) and 5(b)).

DD provided better performance in terms of PIIN elimination by detecting clean chips only. Therefore system performance in terms of BER and SNR is high compared to NAND subtraction. But the drawback of DD is that the complete potential of code weight which corresponds to signal power is not effectively utilized due to detection of only non-overlapping wavelengths. Therefore, BER is affected due to reception of fewer spectral chips which corresponds to less received power.

MAI can be treated well using NAND detection as it subtracts non-overlapping wavelengths but PIIN is still present as it uses full weight in user code sequence. The reason being that, due to increase in code weight PIIN increases linearly in the system causing degradation in system performance. PIIN is introduced in the system due

TABLE 4. Characteristics of QLG and existing codes for various parameters

Code family	Existence	Weight (I)	Cross-correlation (λ)	Code length (N)
RD	$2^M - 1$	Odd	2	$N = K + 2I - 3$
MDW	Even	n	1	$3K + 8/3[\sin(N\pi/3)]^2$
FCC	$K \leq N$	n	$\lambda_c = 2$	$N = IK - \lambda_c(K-1)$
GMP	Optional	Optional	$\lambda_c \leq 1$	$G(N*I)/2$
QLG	Even, odd	$I > 2$	$\lambda_c = 1$	$N = K(I-1)$

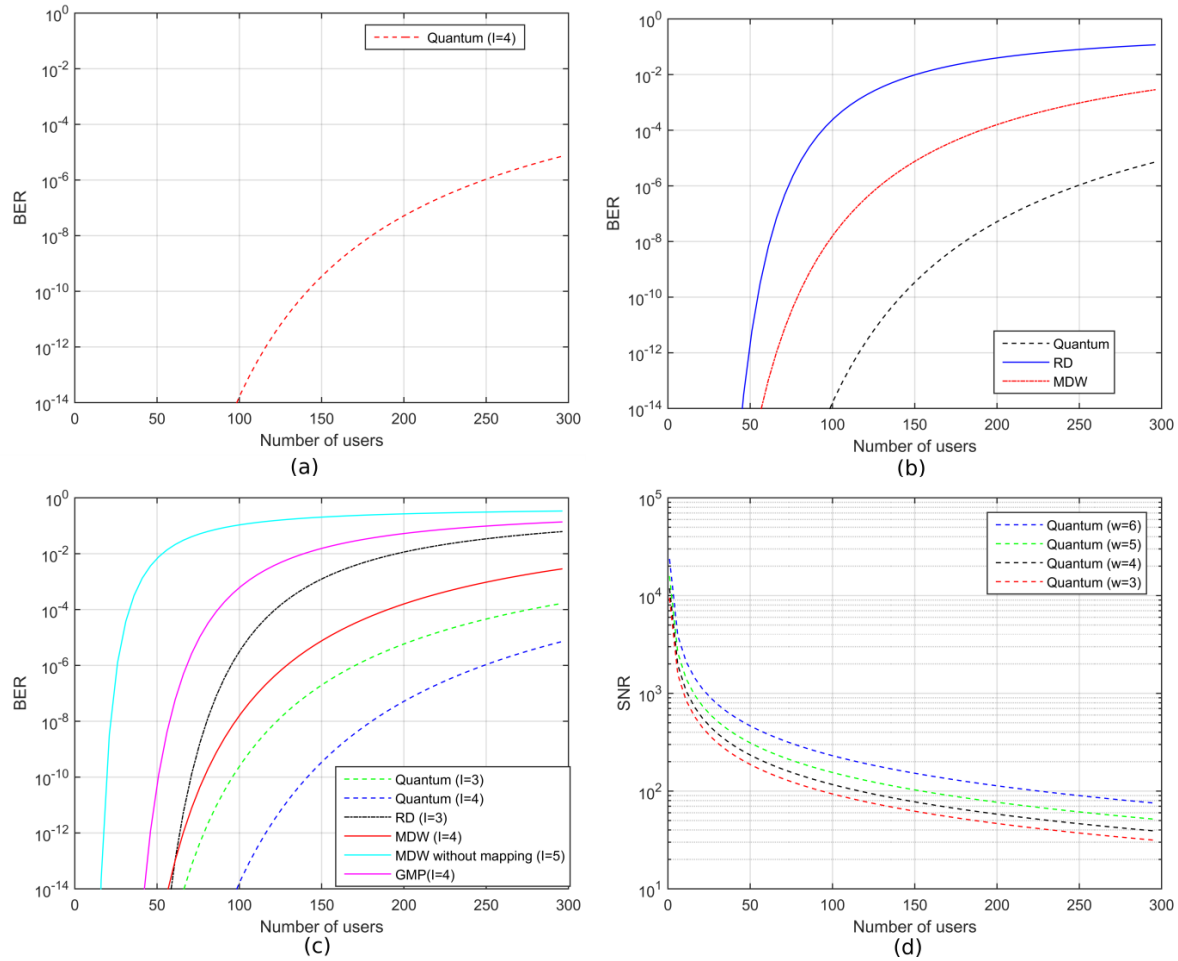


FIG. 4. Dependences of BER and SNR on the number of users (K) at different weights (I) for QLG and existing SAC codes: (a) BER (K) at I = 4, (b) BER(K) for Quantum, RD and MDW at I = 4, (c) BER(K) for RD (I = 3), MDW (I = 4), MDW without mapping (I = 5), GMP (I = 4) and QLG (I = 3, 4) codes, (d) SNR(K) for QLG (I = 3, 4, 5, 6).

to incoherent light fields that are mixed and incident upon the photo diode detector, leading to high intensity noise. High weight corresponds to more intensity noise in the system.

It is also clear that the DD technique supports 120 users while NAND can support 80 simultaneous users at standard error free transmission rate $10e^{-9}$. In the simulation, we also observed that the DD technique reduced cost and system complexity at the receiving end because this technique required fewer filters, PIN diodes and subtractors compared to NAND. As a kind of trade-off between DD and NAND techniques, they can be used based on specific requirement and application. (Figs. 5(c) and 5(d)).

The relations between BER and effective source power received at the receiver (P_{sr}) for varying noise combinations such as Shot-thermal, Shot-thermal and PIIN-thermal are shown in Fig. 6(a). We selected 100 active users for performance comparison. BER changed due to variations in received power. However, BER performance could not be enhanced with the expansion of transmitted power. It was observed that PIIN was the dominating noise in the system

and occurred due to change in amount of received power. PIIN is directly proportional to the number of interfering users and received power is inversely proportional to the quantity of interfering clients and resulted in improvement in BER when P_{sr} exceeded -25 dBm. Shot noise decreased when the amount of received power was high (Fig. 6(a)).

We observed the performance of BER for proposed QLG code at three information rates, 1.25, 2.5 and 5 Gbps (Fig. 6(b)). Results indicated that the data rate increased due to increase in chip rate. Moreover, pulse broadening occurred due to decrease in chip period which was responsible for inter symbol interference phenomena. It was also observed that the number of supportable clients decreased as the information rate increased. In addition, with the expansion of information rate of the framework, BER increased and quantity of supportable clients decreased. This occurred due to increment in data transmission requirement and commotion in framework. Bandwidth requirement is increased with the increase in data rates followed by system noise increment and reduction in number of clients.

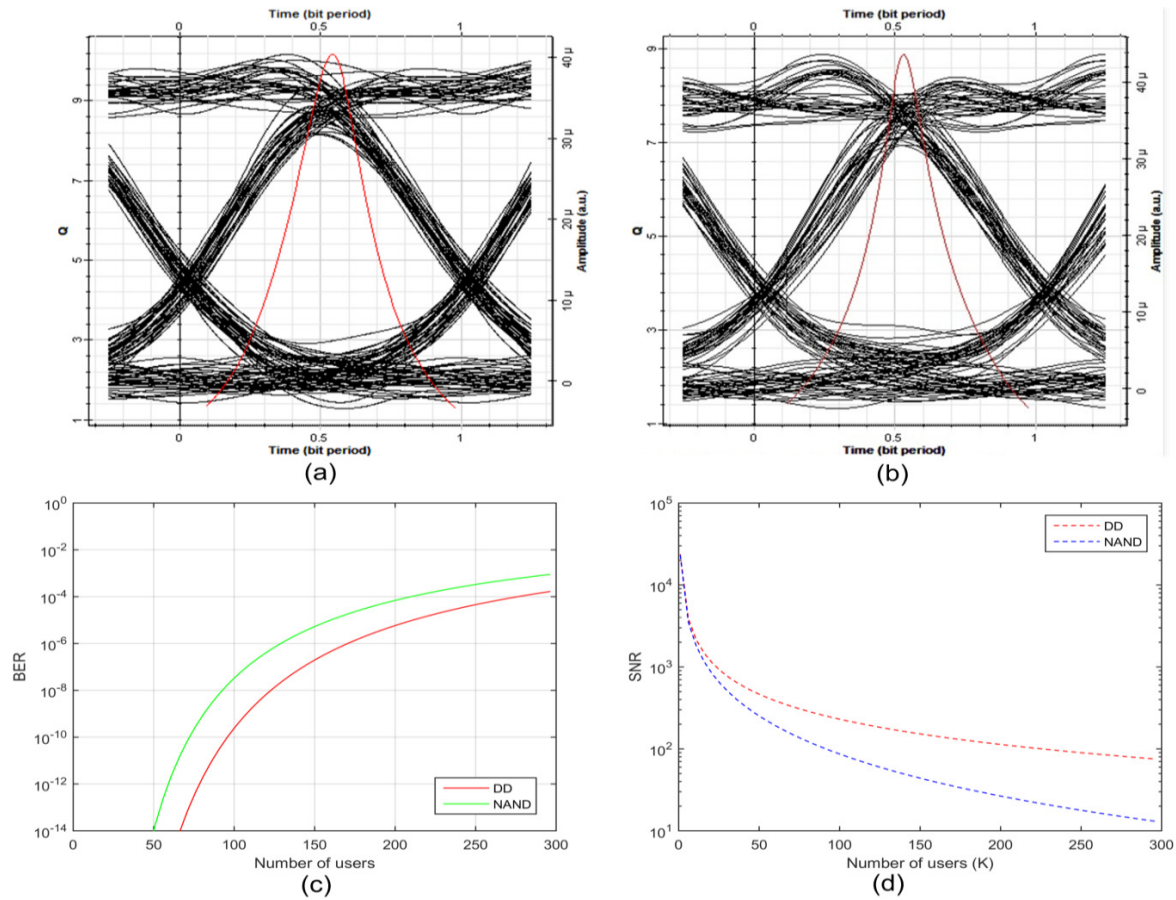


FIG. 5. Examination of QLG code's performance in terms of Q factor, BER and SNR for number of users (K) (a) Q(t) with DD detection (b) Q(t) with NAND technique (c) BER(K) with NAND and DD techniques (d) SNR(K) with NAND and DD techniques.

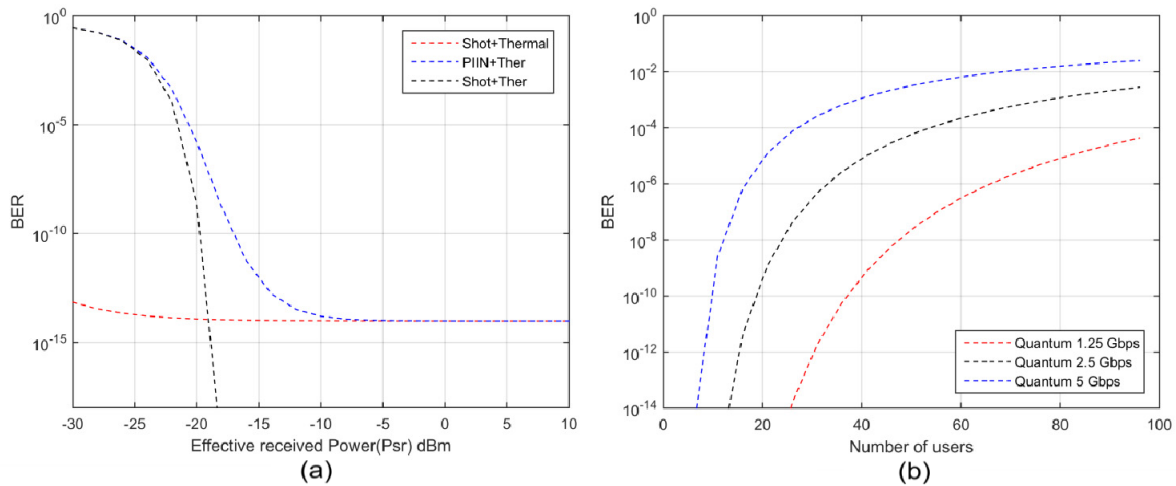


FIG. 6. Relationship between BER, effective received power P_{sr} at ($K = 100, I = 4$) and Number of users (K) for QLG code (a) at (Shot + Ther), (PIIN + Ther) and (Shot + Ther) noises (b) at different data rates.

V. CONCLUSION

In this study, we have designed a new QLG code based on a quantum logic technique for enhancing the execution

of SAC-OCDMA systems. A new algorithm for constructing code was devised. In addition, a quantum logic technique was used for code generation rather than cross correlation to maintain a strategic distance from covering of spectra for

various clients, which dropped the MAI and thus improved performance. The theoretical and simulation result depicted improvement in system performance when compared with other SAC codes (MDW, RD and GMP).

We concluded that the proposed QLG code has the ability to eliminate variable cross-correlation problem when implemented for increased number of users. QLG code may be generated for any weight value greater than 2. The proposed code construction algorithm is free from code mapping. Moreover, for each extended user, constant code length increment was achieved by using QLG code. Further it reduces MAI and PIIN noise effects to a much higher extent due to its ideal in-phase cross-correlation properties ($\lambda_c = 1$), and it improved system performance significantly when employed with a direct detection method. It has an easier code construction method and practical code length which provided good properties for encoder decoder design structure compared to other codes. QLG supports high data-rate transmission in networks. Another important implication of our results is that advanced detection techniques with fewer filters can be designed, which can compensate the cost factor. This work can be further extended to the case of two-dimensional codes associated with broadband and high performance multi-array laser sources [16], in order to achieve higher cardinality and data rates.

REFERENCES

1. N. Kaur, R. Goyal, and M. Rani, "A review on spectral amplitude coding optical code division multiple access," *J. Opt. Commun.* **38**, 77-85 (2017).
2. I. B. Djordjevic and B. Vasic, "Unipolar codes for spectral-amplitude-coding optical CDMA systems based on projective geometries," *IEEE Photon. Technol. Lett.* **15**, 1318-1320 (2003).
3. M. Y. Liu, "Optical CDMA system using spatial AMI coding scheme and coset representative," *Opt. Quantum Electron.* **47**, 503-514 (2015).
4. H. A. Fadhil, S. A. Aljunid, and R. Badlisha, "Triple-play services using random diagonal code for spectral amplitude coding OCDMA systems," *J. Opt. Commun.* **30**, 155-159 (2009).
5. H. Sarangal, A. Singh, J. Malhotra, and S. Chaudhary, "A cost effective 100 Gbps hybrid MDM-OCDMA-FSO transmission system under atmospheric turbulences," *Opt. Quantum Electron.* **49**, 184 (2017).
6. A. M. Alhassan, N. Badruddin, N. M. Saad, and S. A. Aljunid, "Enhancing the performance of coherent sources SAC OCDMA networks via spatial multiplexing," *J. Opt. Soc. Korea* **17**, 471-480 (2013).
7. K. S. Nisar, H. Sarangal, and S. S. Thapar, "Performance evaluation of newly constructed NZCC for SAC-OCDMA using direct detection technique," *Photonic Network Commun.* **37**, 75-82 (2019).
8. M. Z. Norazimah, S. A. Aljunid, H. A. Fadhil, and A. M. Zain, "Analytical comparison of various SAC-OCDMA detection techniques," in *Proc. 2nd IEEE International Conference on Photonics* (Malaysia, Oct. 2011), pp. 1-5.
9. M. Noshad and K. Jamshidi, "Code family for modified spectral-amplitude-coding OCDMA systems and performance analysis," *J. Opt. Commun. Networking* **2**, 344-354 (2010).
10. T. H. Abd, S. A. Aljunid, H. A. Fadhil, R. B. Ahmad, and M. N. Junita, "Enhancement of performance of a hybrid SAC-OCDMA system using dynamic cyclic shift code," *Ukr. J. Phys. Opt.* **13**, 12-27 (2012).
11. S. G. Abdulqader, S. A. Aljunid, H. M. Khafaji, and H. A. Fadhil, "Enhanced performance of SAC-OCDMA system based on SPD detection utilizing EDFA for access networks," *J. Commun.* **9**, 99-106 (2014).
12. Y. Chung, "Design and simulation of two-dimensional OCDMA En/decoder composed of double ring add/drop filters and delay waveguides," *J. Opt. Soc. Korea* **20**, 257-262 (2016).
13. T. Sharma and R. K. Maddila, "Performance characteristics of the spectral amplitude-coding optical CDMA system based on one-dimensional optical codes and a multi-array laser," *Ukr. J. Phys. Opt.* **20**, 81-90 (2019).
14. Y. T. Chang, J. F. Huang, C. T. Yen, C. C. Wang, H. C. Cheng, and K. C. Hsu, "A new shared AWG-based OCDMA scheme implemented with time-spreading and wavelength-group-hopping embedded M-sequence code," *Opt. Fiber Technol.* **16**, 114-123 (2010).
15. M. Y. Liu, "Optical CDMA system using spatial AMI coding scheme and coset representative," *Opt. Quantum Electron.* **47**, 503-514 (2015).
16. T. H. Abd, S. A. Aljunid, H. A. Fadhil, R. A. Ahmad, and N. M. Saad, "Development of a new code family based on SAC-OCDMA system with large cardinality for OCDMA network," *Opt. Fiber Technol.* **17**, 273-280 (2011).
17. M. H. Kakaee, S. Seyedzadeh, H. A. Fadhil, S. B. A. Anas, and M. Mokhtar, "Development of multi-service (ms) for sac-ocdma systems," *Opt. Laser Technol.* **60**, 49-55 (2014).
18. S. A. Aljunid, M. Ismail, A. R. Ramli, B. M. Ali, and M. K. Abdullah, "A new family of optical code sequences for spectral-amplitude-coding optical cdma systems," *IEEE Photon. Technol. Lett.* **16**, 2383-2385 (2004).
19. F. N. Hasoon, S. A. Aljunid, M. K. Abdullah, and S. Shaari, "Spectral amplitude coding OCDMA systems using enhanced double weight code," *J. Eng. Sci. Technol.* **1**, 192-202 (2006).
20. M. K. Abdullah, F. N. Hasoon, S. Aljunid, and S. Shaari, "Performance of OCDMA systems with new spectral direct detection (SDD) technique using enhanced double weight (EDW) code," *Opt. Commun.* **281**, 4658-4662 (2008).
21. N. S. Ahmed, S. A. Aljunid, A. Fadhil, R. B. Ahmad, and M. A. Rashid, "Performance enhancement of OCDMA system using NAND detection with modified double weight (MDW) code for optical access network," *Optik* **124**, 1402-1407 (2013).